

VidEdit: Zero-Shot and Spatially Aware Text-Driven Video Editing

Paul Couairon^{1,3} Clément Rambour² Jean-Emmanuel Haugeard³ Nicolas Thome¹

¹Sorbonne Université, CNRS, ISIR, Paris, France

²Conservatoire National des Arts et Métiers, CEDRIC, Paris, France

³Thales SIX GTS France, Palaiseau, France

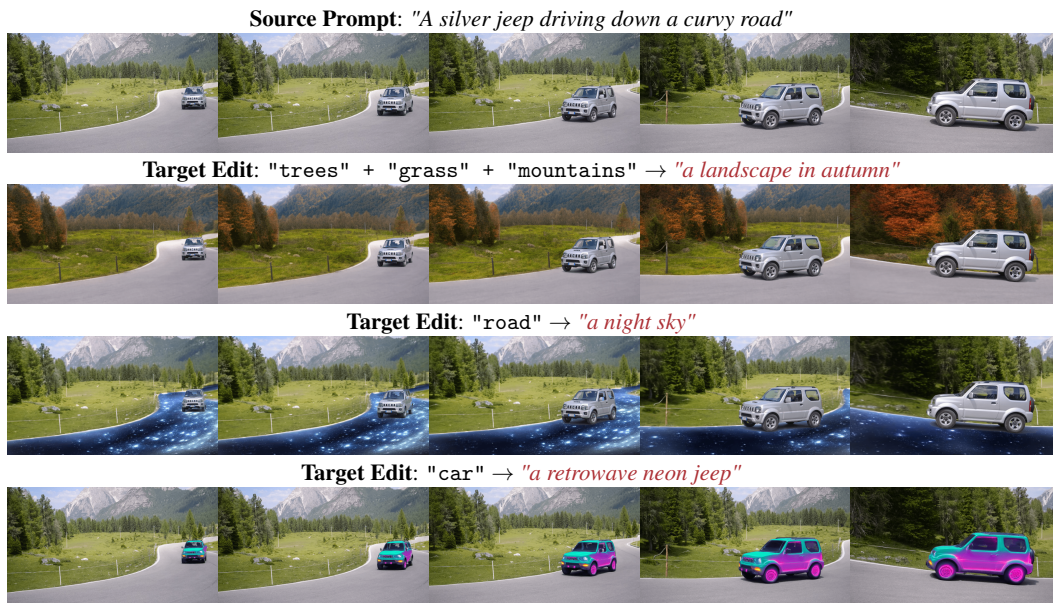


Figure 1: **VIDEDIT** allows to perform rich and diverse video edits on a precise semantic region of interest while perfectly preserving untargeted areas. The method is lightweight and maintains a strong temporal consistency on long-term videos.

Abstract

Recently, diffusion-based generative models have achieved remarkable success for image generation and edition. However, their use for video editing still faces important limitations. This paper introduces **VIDEDIT**, a novel method for zero-shot text-based video editing ensuring strong temporal and spatial consistency. Firstly, we propose to combine atlas-based and pre-trained text-to-image diffusion models to provide a training-free and efficient editing method, which by design fulfills temporal smoothness. Secondly, we leverage off-the-shelf panoptic segmenters along with edge detectors and adapt their use for conditioned diffusion-based atlas editing. This ensures a fine spatial control on targeted regions while strictly preserving the structure of the original video. Quantitative and qualitative experiments show that **VIDEDIT** outperforms state-of-the-art methods on DAVIS dataset, regarding semantic faithfulness, image preservation, and temporal consistency metrics. With this framework, processing a single video only takes approximately one minute, and it can generate multiple compatible edits based on a unique text prompt.

1 Introduction

Diffusion-based models [7, 25, 23, 21] have recently taken over image generation. Contrary to generative adversarial networks [5, 8, 31], they can be reliably trained on massive amounts of data and produce convincing samples. Besides, they can also be used for editing purposes by integrating conditional modalities such as text [23], edge maps or beyond [32, 17]. Such capacities have given rise to numerous methods that assist artists in their content creation endeavor [1, 26, 16, 10].

Yet, unlike image editing, text-based video editing represents a whole new challenge. Naive frame-wise application of text-driven diffusion models leads to flickering video results that look poor to the human eye as they lack motion information and 3D shape awareness. Numerous methods introduce diverse spatio-temporal attention mechanisms that aim to preserve both objects’ appearance across neighboring frames and motion dynamics [28, 19, 3, 27, 13]. However, not only do they require substantial memory resources but also focus on a small number of frames as the proposed attention modules struggle to model long-term dependencies. On the other hand, current atlas-based video editing [2, 14] require costly optimization procedures for each target text query and do not provide precise editing control nor produce diverse samples compatible with a unique text prompt.

In this paper, we introduce **VIDEDIT**, a novel lightweight, and consistent video editing framework that provides object-level control over content. Main steps are illustrated in Fig. 2. We first benefit from Neural Layered Atlas (NLA) [9] to build global representations of the video content which ensure strong spatial and temporal coherence. Second, the underlying scene encoded in the atlas representation is processed through a zero-shot image editing diffusion procedure. Text-based editing inherently faces the difficulty of accurately identifying the region to edit from the input text and may as well deteriorate neighboring regions or introduce rough deformations in the object aspect [28, 3, 13]. We avoid these pitfalls by carefully extracting rich semantic information using HED maps [29] and off-the-shelf segmentation models [4] to guide the diffusion generative process.

Our quantitative and qualitative experiments on DAVIS dataset demonstrate that **VIDEDIT** surpasses atlas-based video baselines as well as video diffusion models when it comes to semantic alignment to the target text query, preserving the original content, and maintaining temporal consistency.

2 VidEdit Framework

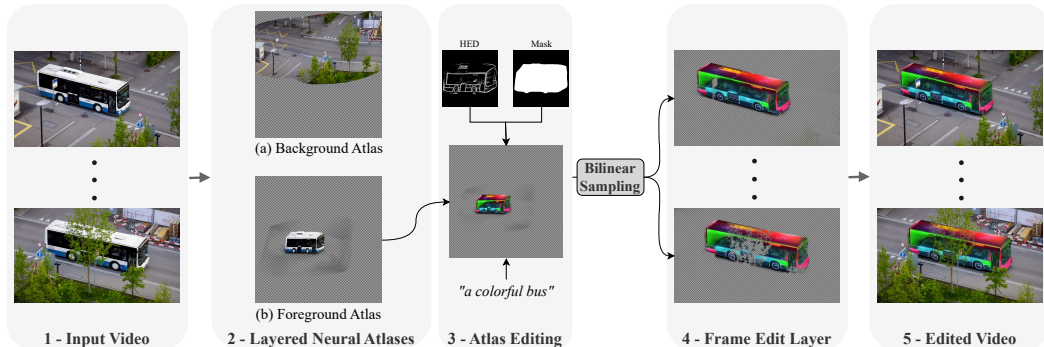


Figure 2: **Our VIDEDIT pipeline:** An input video (1) is fed into NLA models which learn to decompose it into 2D atlases (2). Depending on the object we want to edit, we select an atlas representation onto which we apply our editing diffusion pipeline (3). The edited atlas is then mapped back to frames via a bilinear sampling from the associated pre-trained network \mathbb{M} (4). Finally, the frame edit layers are composited over the original frames to obtain our desired edited video (5).

2D atlas representations pave the way to use off-the-shelf segmentation models [30, 11, 34] for accurately delineating regions of interest. Incorporated into our editing process in Fig. 3, it leads to precise object-level modifications that shows high fidelity with respect to the original video while faithfully rendering the specific target object. In addition, we extract HED maps as they lead to rich object descriptions. We then use the extracted masks to guide the generative process of a latent diffusion model conditioned by both a target prompt and a HED map, the latter ensuring to preserve the semantic structure of the source image.

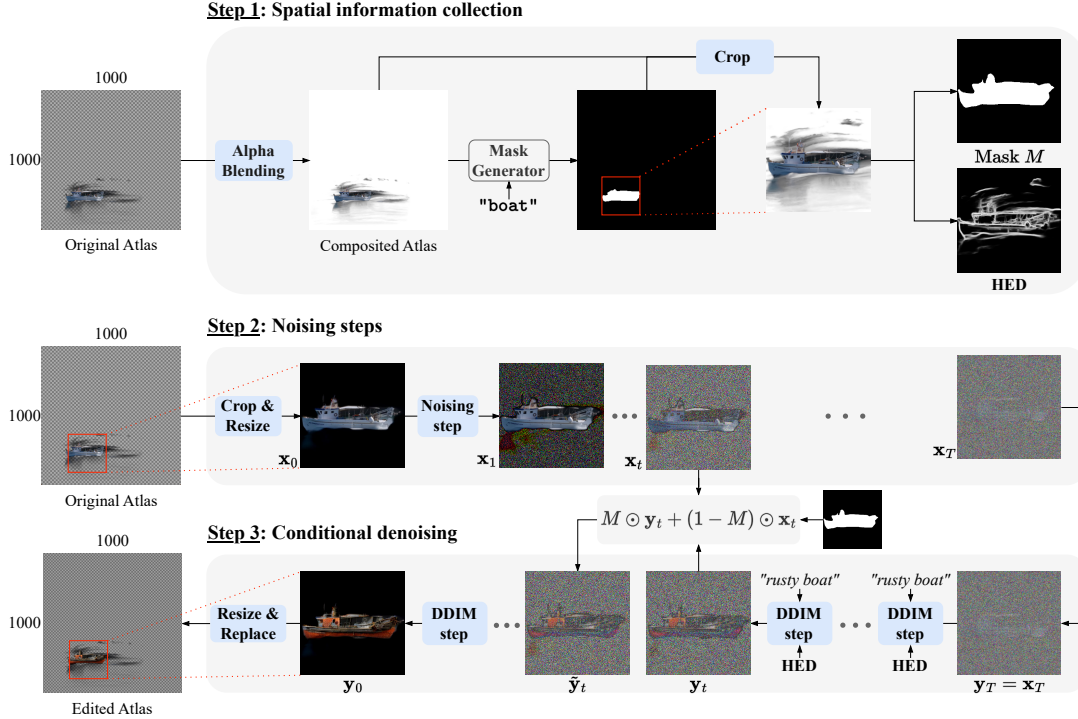


Figure 3: **The three steps of our atlas editing procedure.**

Step 1: Spatial information collection. To confine our edits to the areas of interest and smoothly integrate them into the video content, we leverage a readily available panoptic segmenter. To help it into providing a precise mask (Supplementary E), we blend the RGB values of the atlas with a white patch with respect to its opacity channel. Subsequently, we infer a bounding box around the identified region and recompute a more accurate mask M on this smaller patch. Additionally, we exploit the HED algorithm [29] to bring out critical edges that characterize the structure of our image and that will serve as an external control signal in the generative process to preserve the semantic structure of objects.

Step 2: Noising steps. We crop a patch from the original atlas at the bounding box location to get \mathbf{x}_0 . We use a classical noising procedure for T_{max} steps, which leads to a nearly isotropic Gaussian noise sample $\mathbf{x}_{T_{max}}$, *i.e.* $p_\theta(\mathbf{x}_{T_{max}}) = \mathcal{N}(\mathbf{0}, \mathbf{I})$. We denote ρ the noising ratio such that $\rho = T/T_{max}$.

Step 3: Decoding with mask guidance. We decode our latent \mathbf{y}_T with our diffusion model conditioned on the editing text query, and the extracted HED map. As we use our mask M to guide the diffusion process to preserve exactly the original background, the DDIM update can be written as $\tilde{\mathbf{y}}_{t-1} = M \odot \mathbf{y}_{t-1} + (1 - M) \odot \mathbf{x}_{t-1}$. The edited patch is then resized and replaced in the bounding box. As a result, this pipeline seamlessly fuse the edited region with the unchanged parts of an atlas. Lastly, the edited atlas is queried to sample frame edit layers that, once composited with their corresponding original frames, results in a spatially and temporally consistent edited video.

3 Experiments

In this section, we evaluate our method on videos from DAVIS dataset ranging from 20 to 70 frames. Additional details on the experimental setup and metrics can be found in Supplementary A.

Quantitative results. Sec. 3 gathers the overall comparison with respect to the chosen baselines. Results in bold correspond to the best methods based on a paired t -test (risk 5%). VIDEDIT outperforms other approaches both in semantic and similarity metrics and demonstrates better temporal consistency (C_{Frame}). Additionally, it has a significant advantage, with a ~ 30 -fold speed-up factor over Text2Live in terms of processing time. Supplementary F further illustrates the lightweight aspect of our method. Regarding semantic metrics, as indicated by our directional similarity score (S_{Dir}), VIDEDIT performs highly consistent edits with respect to the change between the target text

query and the source caption. Even though our method is close to Text2Live in terms of frame accuracy ($\mathcal{A}_{\text{Frame}}$) and prompt consistency ($\mathcal{C}_{\text{Prompt}}$), the latter explicitly optimizes a generator on a CLIP-based loss, making these metrics unreliable to assess its generalization performance and editing quality, as shown in Supplementary B.2. Similarity metrics show the capacity of VIDEEDIT to better preserve the visual content of the source video while generating faithful edits to the target queries.

Table 1: **State-of-the-art comparison.**

Method	Semantic				Similarity				Temporal	Time
	$\mathcal{C}_{\text{Prompt}}$ (\uparrow)	$\mathcal{A}_{\text{Frame}}$ (\uparrow)	S_{Dir} (\uparrow)	Agg. Score (\downarrow)	LPIPS (\downarrow)	HaarPSI (\uparrow)	PSNR (\uparrow)	Agg. Score (\downarrow)	$\mathcal{C}_{\text{Frame}}$ (\uparrow)	<i>min</i>
VidEdit (ours)	28.1 (± 3.0)	91.5 (± 11.1)	21.7 (± 8.4)	3.06	0.077 (± 0.054)	0.730 (± 0.109)	22.6 (± 3.6)	3.01	97.4 (± 1.4)	118
Text2Live [2]	28.7 (± 2.8)	94.1 (± 14.6)	20.4 (± 6.0)	3.07	0.155 (± 0.035)	0.710 (± 0.088)	22.8 (± 2.9)	4.04	97.0 (± 1.4)	3780
ControlNet [32]	28.0 (± 2.6)	84.8 (± 24.0)	18.7 (± 6.6)	3.30	0.647 (± 0.061)	0.312 (± 0.036)	10.8 (± 1.5)	12.85	86.2 (± 3.6)	561
SDEdit [15]	26.1 (± 2.9)	65.7 (± 31.8)	14.2 (± 7.4)	3.96	0.490 (± 0.051)	0.377 (± 0.034)	17.9 (± 1.6)	9.57	83.9 (± 5.2)	303
TAV [28]	27.5 (± 3.1)	73.4 (± 36.3)	13.7 (± 9.0)	3.92	0.584 (± 0.079)	0.274 (± 0.060)	13.0 (± 2.1)	12.00	96.4 (± 1.6)	274
Pix2Video [3]	29.0 (± 3.0)	82.9 (± 30.0)	16.2 (± 9.2)	3.47	0.540 (± 0.079)	0.326 (± 0.069)	13.8 (± 2.1)	10.90	94.4 (± 2.1)	252

To further analyze the fine-grained editing capacity of our method while preserving the original content, we display a local $\mathcal{A}_{\text{Frame}}$ score computed within a ground truth mask compared to an outer LPIPS metric (denoted O-LPIPS) computed on the invert of the mask. The size of each dot is proportional to the standard deviation of the local frame accuracy. VIDEEDIT reaches a very good local $\mathcal{A}_{\text{Frame}}$ while showing a huge improvement on the O-LPIPS metric compared to all baselines. This clearly indicates a better preservation of out-of-interest regions.

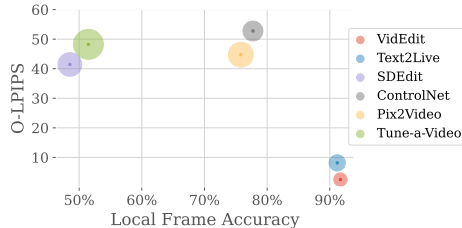


Figure 4: **Masked LPIPS vs Local Object Accuracy**

Ablations. To highlight the importance of our conditional controls, we present a performance comparison in Tab. 2, evaluating our pipeline with mask segmentation and HED conditioning enabled versus scenarios where these controls are turned off. Without any control input, we observe a substantial drop in semantic metrics as the model generates edits randomly across the atlas with shapes that do not align with the target object’s structure. Introducing edge conditioning without spatial awareness closely resembles the previous scenario, with the distinction that the model attempts to achieve local alignment with the control information. This leads to modestly improved semantic and similarity scores. Finally, blending an edit with mask control disregarding edge conditioning produces an edit at the correct location but that is semantically incoherent once mapped back to the original images. Yet, this scenario achieves a decent prompt consistency as the objects still correspond to the target text query. Supplementary C provides a visual illustration of this ablation study.

Table 2: **Ablation study.** The mask and the HED map help to generate meaningful edits once mapped back in the original frame space.

Controls		Semantic metrics			Similarity metrics		
Mask	HED	$\mathcal{C}_{\text{Prompt}}$ (\uparrow)	$\mathcal{A}_{\text{Frame}}$ (\uparrow)	S_{Dir} (\uparrow)	LPIPS (\downarrow)	HaarPSI (\uparrow)	PSNR (\uparrow)
✓	✓	28.1 (± 3.0)	91.5 (± 11.1)	21.7 (± 8.4)	0.077 (± 0.054)	0.730 (± 0.109)	22.6 (± 3.6)
✗	✗	25.5 (± 3.1)	64.3 (± 38.3)	10.6 (± 7.5)	0.099 (± 0.051)	0.632 (± 0.131)	20.1 (± 4.0)
✗	✓	26.3 (± 3.0)	72.4 (± 34.0)	13.0 (± 7.6)	0.095 (± 0.049)	0.672 (± 0.110)	20.8 (± 3.6)
✓	✗	27.5 (± 2.8)	81.9 (± 24.2)	18.0 (± 8.4)	0.081 (± 0.042)	0.639 (± 0.128)	20.7 (± 3.3)

Finally, blending an edit with mask control disregarding edge conditioning produces an edit at the correct location but that is semantically incoherent once mapped back to the original images. Yet, this scenario achieves a decent prompt consistency as the objects still correspond to the target text query. Supplementary C provides a visual illustration of this ablation study.

Diversity. Finally, we illustrate in Fig. 5 the ability of VIDEEDIT to produce diverse edits from a unique pair (*video; text query*). Unlike Text2Live which converges towards a unique solution, our method is able to synthesize more diverse and convincing samples in much less time.



Figure 5: VIDEEDIT and TEXT2LIVE sample diversity.

Future Work. VIDEEDIT is a lightweight algorithm for zero-shot semantic video editing based on latent diffusion models. Experimentally this approach preserves more appearance information from the input video than other diffusion-based methods, leading to lighter edits. Since our method relies on the quality of such atlas representations, one way to expand the scope of possible video edits would be to strengthen and robustify the neural layered atlases construction approach.

References

- [1] Omri Avrahami, Dani Lischinski, and Ohad Fried. Blended diffusion for text-driven editing of natural images. In *2022 IEEE/CVF Conference on Computer Vision and Pattern Recognition (CVPR)*. IEEE, jun 2022. doi: 10.1109/cvpr52688.2022.01767. URL <https://doi.org/10.1109%2Fcvpr52688.2022.01767>.
- [2] Omer Bar-Tal, Dolev Ofri-Amar, Rafail Fridman, Yoni Kasten, and Tali Dekel. Text2live: Text-driven layered image and video editing. In *Computer Vision—ECCV 2022: 17th European Conference, Tel Aviv, Israel, October 23–27, 2022, Proceedings, Part XV*, pages 707–723. Springer, 2022.
- [3] Duygu Ceylan, Chun-Hao Paul Huang, and Niloy J Mitra. Pix2video: Video editing using image diffusion. *arXiv preprint arXiv:2303.12688*, 2023.
- [4] Bowen Cheng, Ishan Misra, Alexander G Schwing, Alexander Kirillov, and Rohit Girdhar. Masked-attention mask transformer for universal image segmentation. In *Proceedings of the IEEE/CVF Conference on Computer Vision and Pattern Recognition*, pages 1290–1299, 2022.
- [5] Ian Goodfellow, Jean Pouget-Abadie, Mehdi Mirza, Bing Xu, David Warde-Farley, Sherjil Ozair, Aaron Courville, and Yoshua Bengio. Generative adversarial networks. *Communications of the ACM*, 63(11):139–144, 2020.
- [6] Jonathan Ho and Tim Salimans. Classifier-free diffusion guidance. *arXiv preprint arXiv:2207.12598*, 2022.
- [7] Jonathan Ho, Ajay Jain, and Pieter Abbeel. Denoising diffusion probabilistic models. *Advances in Neural Information Processing Systems*, 33:6840–6851, 2020.
- [8] Tero Karras, Samuli Laine, and Timo Aila. A style-based generator architecture for generative adversarial networks. *2019 IEEE/CVF Conference on Computer Vision and Pattern Recognition (CVPR)*, pages 4396–4405, 2018.
- [9] Yoni Kasten, Dolev Ofri, Oliver Wang, and Tali Dekel. Layered neural atlases for consistent video editing. *ACM Transactions on Graphics (TOG)*, 40(6):1–12, 2021.
- [10] Bahjat Kawar, Shiran Zada, Oran Lang, Omer Tov, Huiwen Chang, Tali Dekel, Inbar Mosseri, and Michal Irani. Imagic: Text-based real image editing with diffusion models. *arXiv preprint arXiv:2210.09276*, 2022.
- [11] Alexander Kirillov, Eric Mintun, Nikhila Ravi, Hanzi Mao, Chloe Rolland, Laura Gustafson, Tete Xiao, Spencer Whitehead, Alexander C. Berg, Wan-Yen Lo, Piotr Dollár, and Ross B. Girshick. Segment anything. *ArXiv*, abs/2304.02643, 2023.
- [12] Junnan Li, Dongxu Li, Caiming Xiong, and Steven Hoi. Blip: Bootstrapping language-image pre-training for unified vision-language understanding and generation. In *International Conference on Machine Learning*, pages 12888–12900. PMLR, 2022.
- [13] Shaoteng Liu, Yuechen Zhang, Wenbo Li, Zhe Lin, and Jiaya Jia. Video-p2p: Video editing with cross-attention control. *arXiv preprint arXiv:2303.04761*, 2023.
- [14] Sebastian Loeschke, Serge J. Belongie, and Sagie Benaim. Text-driven stylization of video objects. In *ECCV Workshops*, 2022.
- [15] Chenlin Meng, Yutong He, Yang Song, Jiaming Song, Jiajun Wu, Jun-Yan Zhu, and Stefano Ermon. Sdedit: Guided image synthesis and editing with stochastic differential equations. In *International Conference on Learning Representations*, 2021.
- [16] Ron Mokady, Amir Hertz, Kfir Aberman, Yael Pritch, and Daniel Cohen-Or. Null-text inversion for editing real images using guided diffusion models. *arXiv preprint arXiv:2211.09794*, 2022.
- [17] Chong Mou, Xintao Wang, Liangbin Xie, Jing Zhang, Zhongang Qi, Ying Shan, and Xiaohu Qie. T2i-adapter: Learning adapters to dig out more controllable ability for text-to-image diffusion models. *ArXiv*, abs/2302.08453, 2023.

- [18] Jordi Pont-Tuset, Federico Perazzi, Sergi Caelles, Pablo Arbeláez, Alex Sorkine-Hornung, and Luc Van Gool. The 2017 davis challenge on video object segmentation. *arXiv preprint arXiv:1704.00675*, 2017.
- [19] Chenyang Qi, Xiaodong Cun, Yong Zhang, Chenyang Lei, Xintao Wang, Ying Shan, and Qifeng Chen. Fatezero: Fusing attentions for zero-shot text-based video editing. *arXiv preprint arXiv:2303.09535*, 2023.
- [20] Alec Radford, Jong Wook Kim, Chris Hallacy, Aditya Ramesh, Gabriel Goh, Sandhini Agarwal, Girish Sastry, Amanda Askell, Pamela Mishkin, Jack Clark, et al. Learning transferable visual models from natural language supervision. In *International conference on machine learning*, pages 8748–8763. PMLR, 2021.
- [21] Aditya Ramesh, Prafulla Dhariwal, Alex Nichol, Casey Chu, and Mark Chen. Hierarchical text-conditional image generation with clip latents. *arXiv preprint arXiv:2204.06125*, 2022.
- [22] Rafael Reisenhofer, Sebastian Bosse, Gitta Kutyniok, and Thomas Wiegand. A haar wavelet-based perceptual similarity index for image quality assessment. *Signal Processing: Image Communication*, 61:33–43, 2018. ISSN 0923-5965. doi: <https://doi.org/10.1016/j.image.2017.11.001>. URL <https://www.sciencedirect.com/science/article/pii/S0923596517302187>.
- [23] Robin Rombach, Andreas Blattmann, Dominik Lorenz, Patrick Esser, and Björn Ommer. High-resolution image synthesis with latent diffusion models. In *Proceedings of the IEEE/CVF Conference on Computer Vision and Pattern Recognition*, pages 10684–10695, 2022.
- [24] Christoph Schuhmann, Romain Beaumont, Richard Vencu, Cade Gordon, Ross Wightman, Mehdi Cherti, Theo Coombes, Aarush Katta, Clayton Mullis, Mitchell Wortsman, et al. Laion-5b: An open large-scale dataset for training next generation image-text models. *arXiv preprint arXiv:2210.08402*, 2022.
- [25] Jiaming Song, Chenlin Meng, and Stefano Ermon. Denoising diffusion implicit models. *arXiv preprint arXiv:2010.02502*, 2020.
- [26] Narek Tumanyan, Michal Geyer, Shai Bagon, and Tali Dekel. Plug-and-play diffusion features for text-driven image-to-image translation. *arXiv preprint arXiv:2211.12572*, 2022.
- [27] Wen Wang, Kangyang Xie, Zide Liu, Hao Chen, Yue Cao, Xinlong Wang, and Chunhua Shen. Zero-shot video editing using off-the-shelf image diffusion models. *arXiv preprint arXiv:2303.17599*, 2023.
- [28] Jay Zhangjie Wu, Yixiao Ge, Xintao Wang, Weixian Lei, Yuchao Gu, Wynne Hsu, Ying Shan, Xiaohu Qie, and Mike Zheng Shou. Tune-a-video: One-shot tuning of image diffusion models for text-to-video generation. *arXiv preprint arXiv:2212.11565*, 2022.
- [29] Saining Xie and Zhuowen Tu. Holistically-nested edge detection. In *Proceedings of the IEEE international conference on computer vision*, pages 1395–1403, 2015.
- [30] Jiarui Xu, Sifei Liu, Arash Vahdat, Wonmin Byeon, Xiaolong Wang, and Shalini De Mello. Open-vocabulary panoptic segmentation with text-to-image diffusion models. *ArXiv*, abs/2303.04803, 2023.
- [31] Jiahui Yu, Xin Li, Jing Yu Koh, Han Zhang, Ruoming Pang, James Qin, Alexander Ku, Yuanzhong Xu, Jason Baldridge, and Yonghui Wu. Vector-quantized image modeling with improved vqgan. *arXiv preprint arXiv:2110.04627*, 2021.
- [32] Lvmin Zhang and Maneesh Agrawala. Adding conditional control to text-to-image diffusion models. *arXiv preprint arXiv:2302.05543*, 2023.
- [33] Richard Zhang, Phillip Isola, Alexei A Efros, Eli Shechtman, and Oliver Wang. The unreasonable effectiveness of deep features as a perceptual metric. In *Proceedings of the IEEE conference on computer vision and pattern recognition*, pages 586–595, 2018.
- [34] Xueyan Zou, Jianwei Yang, Hao Zhang, Feng Li, Linjie Li, Jianfeng Gao, and Yong Jae Lee. Segment everything everywhere all at once. *ArXiv*, abs/2304.06718, 2023.

VidEdit: Zero-shot and Spatially Aware Text-driven Video Editing

Supplementary Material

A Experimental Setup

Dataset. Following [2, 28, 19], we evaluate our approach on videos from DAVIS dataset [18] resized at a 768×432 resolution. The length of these videos ranges from 20 to 70 frames. To automatically create edit prompts, we use a captioning model [12] to obtain descriptions of the original video content and we manually design 4 editing prompts for each video.

VidEdit setup. Our experiments are based on latent diffusion models [23]. We use a version of stable diffusion trained with HED edge detection [32] at a 512×512 resolution on LAION-5B dataset [24]. We choose Mask2former [4] as our instance segmentation network. To edit an atlas, we sample pure Gaussian noise (*i.e.* $\rho = 1$) and denoise it for 50 steps with DDIM sampling and classifier-free guidance [6]. For a single 70 frames video, it takes ~ 15 seconds to edit a 512×512 patch in an atlas and ~ 1 minute to reconstruct the video with the edit layer on a NVIDIA TITAN RTX. We set up the HED strength λ to 1 by default.

Baselines. We compare our method with two text-to-image frame-wise editing approaches and three text-to-video editing baselines.

1. *SDEdit* [15] is a framewise zero-shot editing approach that corrupts an input frame with noise and denoise it with a target text prompt.
2. *ControlNet* [32] performs frame-wise editing with an external condition extracted from the target frame.
3. *Text2Live* [2] is a Neural Layered Atlas (NLA) based method that trains a generator for each text query to optimize a CLIP-based loss.
4. *Tune-a-Video* (TAV) [28] fine-tunes an inflated version of a pre-trained diffusion model on a video to produce similar content.
5. *Pix2Video* [3] uses a structure-guided image diffusion model to perform text-guided edits on a key frame and propagate the changes to the future frames via self-attention feature injection.

Metrics. A video edit is expected to (1) be temporally consistent (**Temporal**), (2) faithfully render a target text query (**Semantics**) and (3) preserve out-of-interest regions unaltered (**Similarity**). To evaluate CLIP based metrics, we used CLIP ViT-L/14 [20].

- **Temporal**

- **Frame Consistency (C_{Frame}).** Assesses the temporal coherence of a video. It measures the CLIP similarity between consecutive video frames.

$$C_{\text{Frame}} = \frac{1}{N} \sum_{k=1}^N \frac{1}{F_k} \sum_{j=1}^{F_k-1} \text{CLIPScore}(\bar{I}_j^k, \bar{I}_{j+1}^k)$$

where \bar{I}_j^k is the j -th frame of edited video k , F_k the number of frames in video k and N the number of edited videos.

- **Semantics**

- **Prompt Consistency** ($\mathcal{C}_{\text{Prompt}}$). Measures the average CLIP similarity between a target text query and each video frame.

$$\mathcal{C}_{\text{Prompt}} = \frac{1}{N} \sum_{k=1}^N \frac{1}{F_k} \sum_{j=1}^{F_k} \text{CLIPScore}(\bar{I}_j^k, \bar{C}^k)$$

with \bar{C}^k the edited caption of video k .

- **Frame Accuracy** ($\mathcal{A}_{\text{Frame}}$). Corresponds to the average percentage of edited frames that have a higher CLIP similarity with the target text query than with their source caption.

$$\mathcal{A}_{\text{Frame}} = \frac{1}{N} \sum_{k=1}^N \frac{1}{F_k} \sum_{j=1}^{F_k} \mathbb{1}\{\text{CLIPScore}(\bar{I}_j^k, \bar{C}^k) > \text{CLIPScore}(\bar{I}_j^k, C^k)\} \times 100$$

- **Directional Similarity** (\mathcal{S}_{Dir}). Quantifies how closely the alterations made to an original image align with the changes between the source and target caption. For a single frame the similarity score writes: $\text{SIMScore}(\bar{I}_j^k, I_j^k, \bar{C}^k, C^k) = 100 * \cos(E_{\bar{I}_j^k} - E_{I_j^k}, E_{\bar{C}^k} - E_{C^k})$.

$$\mathcal{S}_{\text{Dir}} = \frac{1}{N} \sum_{k=1}^N \frac{1}{F_k} \sum_{j=1}^{F_k} \text{SIMScore}(\bar{I}_j^k, I_j^k, \bar{C}^k, C^k)$$

- **Similarity**

Regarding content preservation, we have chosen three metrics that operate on different feature spaces in order to capture a rich description of perceptual similarities.

- **LPIPS** [33] operates on the deep feature space of a VGG network and has been shown to match human perception well.
- **HaarPSI** [22] While LPIPS evaluates the perceptual similarity between two images in a deep feature space, HaarPSI performs a Haar wavelet decomposition to assess local similarities.
- **PSNR** measures the distance with an original image in the pixel space.

These metrics are extensively described in the literature and we refer to it for further details.

- **Aggregate Score.**

This metric synthesizes in a single score the overall performance of each model on semantic and similarity aspects, relatively to the best baseline. When dealing with metrics where a higher value is considered preferable, a coefficient in the aggregate score is computed as: $\max(\mathcal{S}_i)/\mathcal{S}_i^j$ i.e. the best score for metric i divided by the score of baseline j for metric i . When the objective is to minimize the metric, we take the inverse value. The minimal and best aggregate score for each aspect is 3, as we aggregate three semantic or similarity scores.

B Qualitative Results

B.1 VIDEEDIT samples

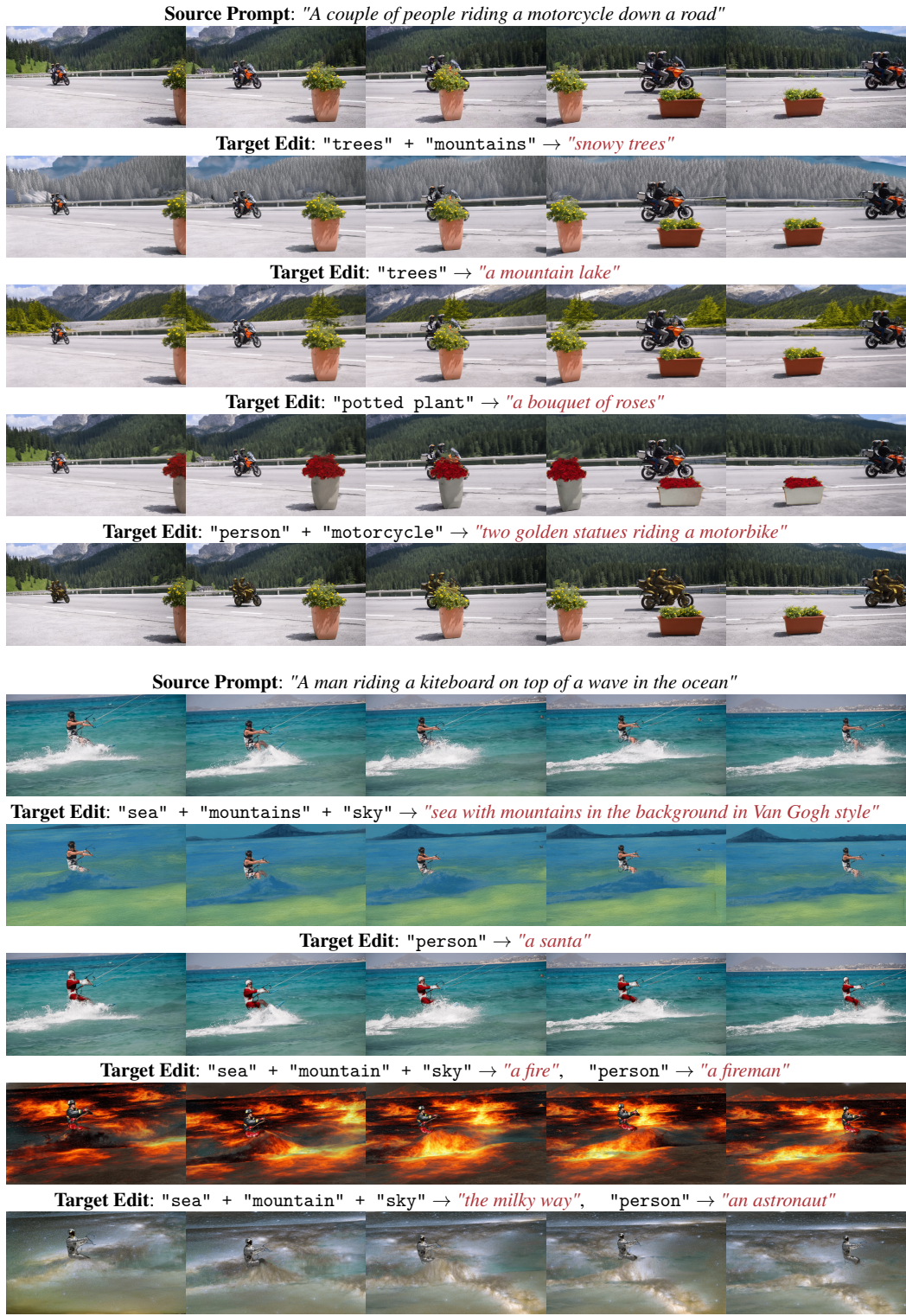


Figure 6: Additional VIDEEDIT sample results.

B.2 Comparison against baselines

We show in Fig. 7 a visual comparison against the baselines to qualitatively assess the improvement brought out by our method. We can see that VIDEEDIT performs fine-grained editing while perfectly preserving out-of-interest regions. In comparison to other baselines, the edits generated are more visually appealing and realistic. For example, VIDEEDIT obtains a frame accuracy ($\mathcal{A}_{\text{Frame}}$) and prompt consistency ($\mathcal{C}_{\text{Prompt}}$) scores of 26.5 and 30 respectively compared to Text2Live which reaches 26 and 35 respectively. However, we can see that Text2Live’s scores do not automatically translate into high-quality edits it often struggles to render detailed textures precisely localized on targeted regions. For example, ice creams are poorly rendered and some untargeted areas are being altered. Regarding Tune-a-Video and Pix2Video baselines, the methods are unable to generate a faithful edit at the exact location and completely degrade the original content. Despite relatively high frame consistency scores in this video (96% for Tune-a-Video and 89% for Pix2Video vs 97.5% for VIDEEDIT), noticeable flickering artifacts undermine the video content. On the other hand, naive frame-wise application of image-to-image translation methods also leads to temporally inconsistent results. For example, SDEdit is unable to both generate a faithful edit and to preserve the original content as it inherently faces a trade-off between the two.

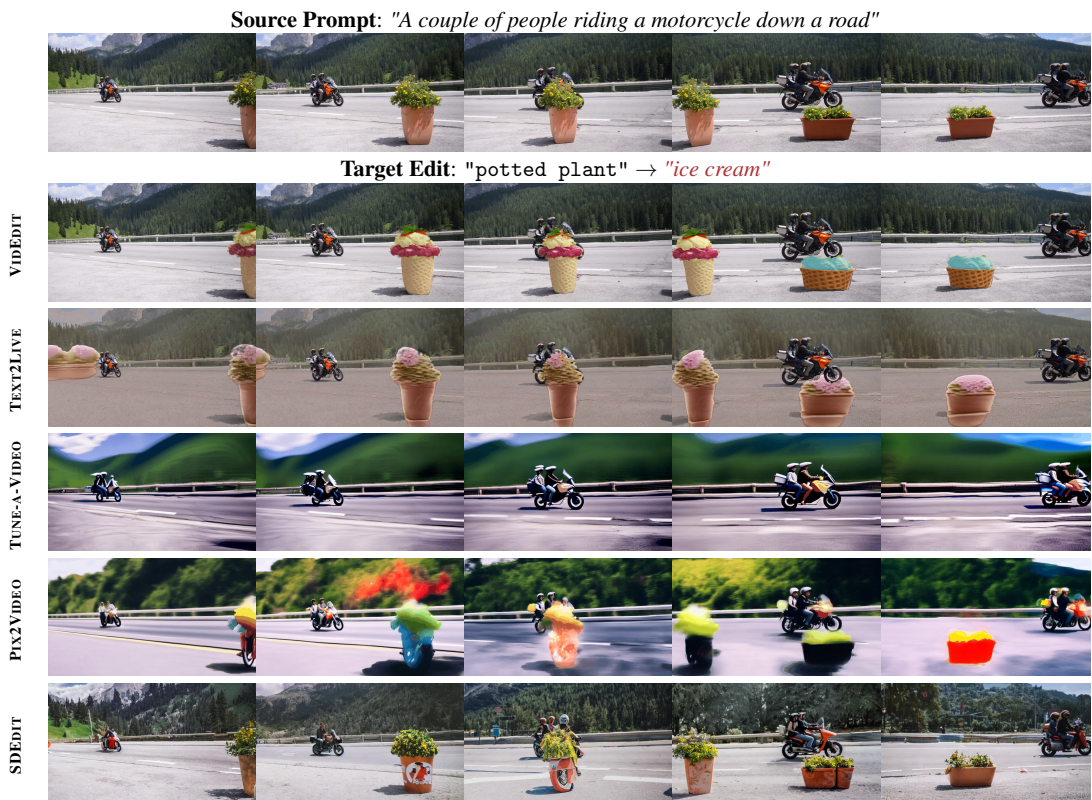


Figure 7: **Qualitative comparison of VIDEEDIT with other baselines.**VIDEEDIT generates higher quality textures than Text2Live. Tune-a-Video and Pix2video completely alters untargeted regions.

Fig. 8 shows additional baselines comparison examples. We can see on both videos that VIDEEDIT renders more realistic and higher quality textures than other methods while perfectly preserving the original content outside the regions of interest. The flamingo has subtle grooves on its body that imitate feathers and a fine light effect enhances the edit's grain. On the contrary, Text2Live struggles to render a detailed plastic appearance. The generated wooden boat also looks less natural and more tarnished than VIDEEDIT's. Tune-a-Video and Pix2Video render unconvincing edits and completely alters the original content.

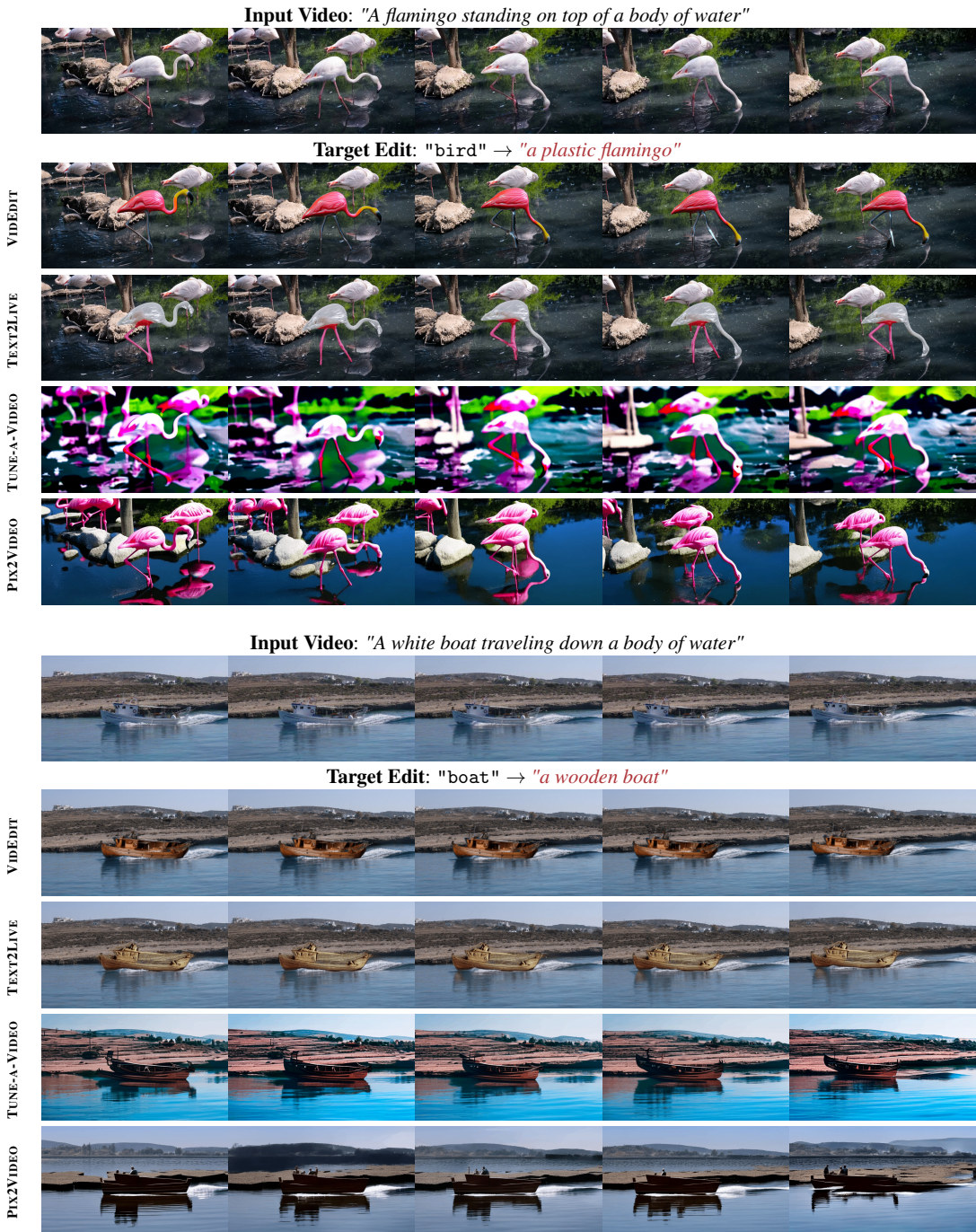


Figure 8: Additional qualitative comparison between baselines.

C Ablation Visualization

Fig. 9 illustrates the ablation study we led in Tab. 2. When VIDEEDIT receives both conditional controls, it produces high quality results. Conversely, when these controls are deactivated, the model is free to perform edits at random locations in the atlas, resulting in uninterpretable visual outcomes. Enabling only the edge conditioning yields similar results, with the difference that the model attempts to locally match inner and outer edges. Finally, the sole use of a mask allows to perform edits at the correct locations, but that are semantically absurd once mapped back to the image space. We provide additional qualitative results in this anonymous git repository <https://anonymous.4open.science/r/videdit-videos-1BDC>



Figure 9: Ablation visualization.

D Model Analysis

Impact of hyperparameters. We analyze in Fig. 10 VIDEEDIT’s behaviour versus the HED conditioning strength and noising ratio, respectively λ and ρ . To analyze the trade-off between semantic editing and source image preservation, we compute a local LPIPS computed within a ground-truth mask, provided by DAVIS, versus a local CLIP score computed within the same mask for an edited object.

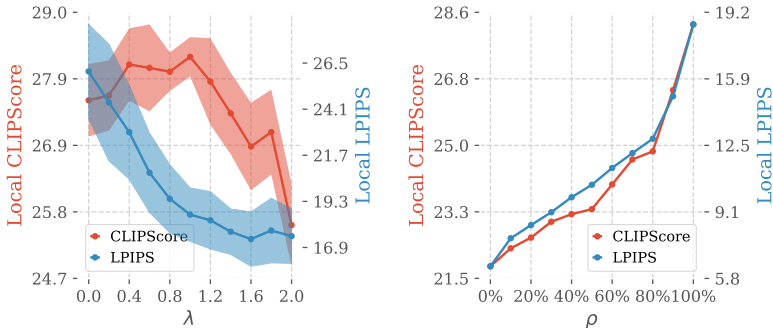


Figure 10: VIDEEDIT behavior wrt. different λ and ρ values.

On the left panel, we can see that for λ values lower than 0.4, the edge conditioning is not strong enough to guide the edits toward a plausible output on the video frames. This phenomenon is illustrated in Supplementary C. On the contrary, for strength values larger than 1.2, the conditioning weighs too much on the model and hinders its ability to generate faithful edits. As expected, we notice that the local LPIPS decreases as the edge conditioning increases. While the decreasing rate is substantial between 0 and 1, the marginal gain diminishes for larger values. Overall, setting the HED strength between 0.8 and 1.2 robustly enables to both perform faithful edits and preserve the original content. On the right panel, we see that both local CLIP score and LPIPS increase with the noising ratio. Indeed, for a null ρ value, the region is reconstructed from the atlas, nearly identically to the original, and is then rewarded a low LPIPS. However, as no modification has been performed, the patch does not match the target text query and gets a lower CLIP score. As the noising ratio increases, the region deviates more from the input but also better matches the target edit. Note that for a ρ value of 100%, the local LPIPS is constrained below 19, which still indicates a low disparity with the original image.

E Blending Effect

Fig. 11 shows the blending step’s importance in the editing pipeline (Fig. 3). When considering only the RGB channels of a foreground atlas to infer an object’s mask, the segmentation network has to deal with low contrasts between the background and the object, as well as duplicated representations within the overall atlas representation. This might lead to partially detected objects or masks placed at an incorrect location. In order to avoid these pitfalls, we leverage the atlas’ alpha channel which indicates which pixels contain relevant information and must thus be visible. Therefore, we choose to blend the RGB channels with a fully white image according to the alpha values:

$$\mathbb{A}_{\text{Blended}} = \mathbb{A}_{\text{RGB}} \odot \alpha + \mathbb{I} \odot (1 - \alpha)$$

with \mathbb{A}_{RGB} the RGB channels of an atlas representation, \mathbb{I} a fully white image and α the atlas’ opacity values.

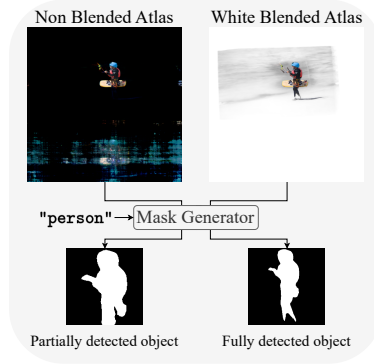


Figure 11: Alpha blending effect

F Editing Time

Focusing on the iterative part of editing¹ in which users are interested in², Figure 12 underlines the lightweight aspect of our method. The panel on the left shows that VIDEEDIT can perform a large number of edits on a 70 frame long video in significantly less time than other approaches. As an illustration, VIDEEDIT demonstrates approximately 30 times faster editing capabilities compared to Text2Live, which is the second leading baseline in terms of editing capacities. On the other hand, as depicted in the right panel, the use of VIDEEDIT becomes increasingly time-efficient compared to other baselines, as the number of frames to edit grows.

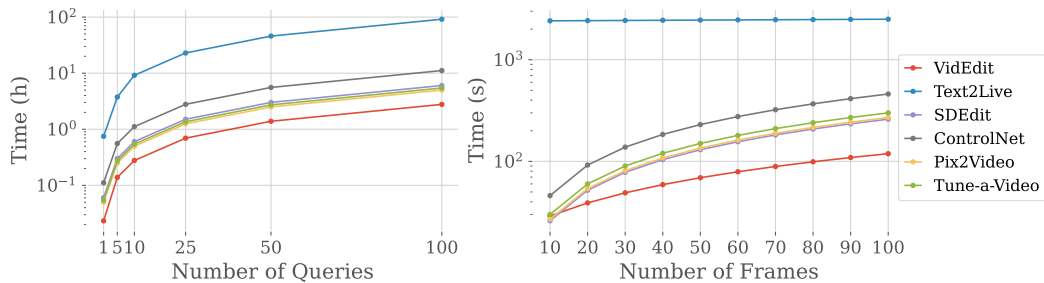


Figure 12: **Editing time.** VIDEEDIT can edit videos significantly faster than existing methods.

¹Steps as DDIM inversion or LNA construction being considered as pre-processing steps.

²Editing the atlas and reconstructing the video for atlas based methods. Simply inferring the model for other baselines.